

# Characterization of calcium-binding sites in the kidney stone inhibitor glycoprotein nephrocalcin with vanadyl ions: Electron paramagnetic resonance and electron nuclear double resonance spectroscopy

DEVKUMAR MUSTAFI\* AND YASUSHI NAKAGAWA

Department of Biochemistry and Molecular Biology, University of Chicago, Cummings Life Science Center, 920 East 58th Street, Chicago, IL 60637

Communicated by Clyde A. Hutchison, Jr., July 25, 1994 (received for review April 26, 1994)

**ABSTRACT** Nephrocalcin (NC) is a calcium-binding glycoprotein of 14,000 molecular weight. It inhibits the growth of calcium oxalate monohydrate crystals in renal tubules. The NC used in this study was isolated from bovine kidney tissue and purified with the use of DEAE-cellulose chromatography into four isoforms, designated as fractions A–D. They differ primarily according to the content of phosphate and  $\gamma$ -carboxyglutamic acid. Fractions A and B are strong inhibitors of the growth of calcium oxalate monohydrate crystal, whereas fractions C and D inhibit crystal growth weakly. Fraction A, with the highest  $\text{Ca}^{2+}$ -binding affinity, was characterized with respect to its metal-binding sites by using the vanadyl ion ( $\text{VO}^{2+}$ ) as a paramagnetic probe in electron paramagnetic resonance (EPR) and electron nuclear double resonance (ENDOR) spectroscopic studies. By EPR spectrometric titration, it was shown that fraction A of NC bound  $\text{VO}^{2+}$  with a stoichiometry of metal:protein binding of 4:1. Also, the binding of  $\text{VO}^{2+}$  to NC was shown to be competitive with  $\text{Ca}^{2+}$ . Only protein residues were detected by proton ENDOR as ligands, and these ligands bound with complete exclusion of solvent from the inner coordination sphere of the metal ion. This type of metal-binding environment, as derived from  $\text{VO}^{2+}$ -reconstituted NC, differs significantly from the binding sites in other  $\text{Ca}^{2+}$ -binding proteins.

Nephrocalcin (NC), a calcium-binding glycoprotein of 14,000 molecular weight, is known to inhibit growth of calcium oxalate monohydrate (COM) crystals in renal tubules (1). This inhibitor protein has been isolated in four isoforms from urine of normal subjects (1) and kidney stone patients (2), from surgically removed calcium oxalate kidney stones (3), and from kidney tissue of nine species of vertebrates (4). Among these nine species, the dissociation constant of these inhibitor proteins for binding COM crystals varies from  $6 \times 10^{-6}$  to  $4 \times 10^{-8}$  M. Purification of NC from bovine kidney tissue by DEAE-cellulose chromatography showed that it also consists of four isoforms, which have been designated as fractions A–D (4–6). Fractions A–D of NC were also obtained similarly from other species, as described earlier (1–4). Fractions A and B, the “strong” inhibitors, are abundant in normal subjects (1), whereas stone formers excrete less of fractions A and B and more of C and D, which are “weak” inhibitors (2). NC is an acidic glycoprotein containing 33% acidic amino acid residues (Asp and Glu) and about 5% aromatic and basic amino acid residues (5). Fractions A–D differ according to the content of carbohydrate and phosphate. Also, the strong inhibitors contain three or four  $\gamma$ -carboxyglutamic acid residues per molecule, which are not present in NC of stone-forming patients (5).

We have previously shown that, on the basis of  $^{31}\text{P}$  NMR studies of  $\text{Ca}^{2+}$ -NC complexes and by equilibrium dialysis with  $^{45}\text{Ca}$ , a total of 4 mol of  $\text{Ca}^{2+}$  are bound per mol of NC (6). In this study we characterized the metal-binding properties of normal NC<sup>†</sup> (fraction A) by EPR and electron nuclear double resonance (ENDOR) using the vanadyl ion ( $\text{VO}^{2+}$ ) as a paramagnetic probe. The  $\text{VO}^{2+}$  ion has been shown to be an effective paramagnetic substitute for many divalent metal ions in metalloproteins and metalloenzymes (7–10) and is, in particular, an effective substitute for  $\text{Ca}^{2+}$  and  $\text{Mg}^{2+}$  (11, 12).  $\text{VO}^{2+}$  is an ideal substitute for  $\text{Ca}^{2+}$  because  $\text{VO}^{2+}$ , like  $\text{Ca}^{2+}$ , has a high affinity for binding to oxygen-donor ligands (7). By EPR spectrometric titration, we have shown that  $\text{VO}^{2+}$  binds to NC-A with a stoichiometry of 4 mol/mol of protein. Furthermore, we have also demonstrated that  $\text{VO}^{2+}$  competes with  $\text{Ca}^{2+}$  in binding to NC. An unusual result of this preliminary study of  $\text{VO}^{2+}$ -NC complexes obtained by ENDOR spectroscopy showed that the coordinating ligands to the metal ions are from protein residues with complete exclusion of solvent water from the inner coordination sphere.

## EXPERIMENTAL PROCEDURES

**Materials.** NC was isolated from fresh bovine kidney tissue and separated into four fractions by DEAE-cellulose chromatography (Whatman DE-52), as described (1). These fractions were eluted by varying the ionic strength: NC-A at 10–15 mS, NC-B at 16–23 mS, NC-C at 24–27 mS, and NC-D at 32–38 mS, using a linear gradient of NaCl from 0.1 M to 0.5 M in 0.05 M Tris-HCl at pH 7.3. Fraction A (NC-A<sup>†</sup>), which exhibits the highest affinity for  $\text{Ca}^{2+}$  binding, was used in this study. This fraction of protein has been found in normal (non-kidney stone) subjects and can be used as a model system for a strong inhibitor protein. Fraction A of NC was first eluted at a conductivity between 10 and 12 mS and then further purified by Sephacryl S-200 gel filtration chromatography (Pharmacia LKB,  $2 \times 100$  cm) with 0.05 M Tris-HCl buffer at pH 7.3 containing 0.2 M NaCl and 0.02% sodium azide. Chromatographically purified NC-A was dialyzed and lyophilized and then dissolved in 0.03 M Pipes at pH 5.8 to a concentration of 12–14 mg/ml for spectroscopic studies. This solution was then treated with Chelex-100 by dialysis to ensure removal of metal ions. Metal ion removal (mostly  $\text{Ca}^{2+}$ ) was confirmed by atomic absorption (1).

Abbreviations: COM, calcium oxalate monohydrate; ENDOR, electron nuclear double resonance; hf, hyperfine; NC, nephrocalcin; NC-A, fraction A of NC.

\*To whom reprint requests should be addressed.

<sup>†</sup>Since this study is primarily with use of normal NC, the abbreviation NC is often used for normal NC (fraction A). The three other fractions B–D, if used, are always abbreviated as NC-B, NC-C, and NC-D, respectively.

The publication costs of this article were defrayed in part by page charge payment. This article must therefore be hereby marked “advertisement” in accordance with 18 U.S.C. §1734 solely to indicate this fact.

**Methods. Chemical Analyses.** Protein concentration was determined by alkaline hydrolysis followed by the ninhydrin color reaction at 570 nm (1) using bovine serum albumin as a standard. Phosphate content was determined by the modified Fiske–Subbarow method after ashing and hydrolysis (13). Carbohydrate analysis was accomplished by gas chromatography after hydrolysis in 1 M HCl/methanol at 80°C for 24 hr followed by neutralization and trimethylsilylation as described by Clamp *et al.* (14).

Molecular weight was estimated from the elution profile of Sephacryl S-200 column chromatography calibrated with bovine serum albumin (68,000), carbonic anhydrase (29,000), soybean trypsin inhibitor (21,000), and lysozyme (14,000). Properties of NC-A are summarized in Table 1.

**CD.** CD spectra of NC in the absence or presence of  $\text{VO}^{2+}$  and  $\text{Ca}^{2+}$  ions were recorded with a JASCO J-600 CD spectropolarimeter. NC-A was diluted to 0.20 mg/ml of protein with 0.03 M Pipes at pH 5.8. The protein solution was then titrated with freshly prepared  $\text{VO}_2\text{SO}_4$  solution to the desired ratio of  $[\text{VO}^{2+}]:[\text{NC}]$ . CD spectra in the far-ultraviolet region were measured for samples using a 1-mm light pathlength and were the average of three spectral scans. For the calculation of molar ellipticity  $[\Theta]$ , a mean residue weight of 110 was used. The CD intensities were calibrated by using an aqueous solution containing 0.06% (1S)-(+)-10-camphorsulfonic acid.

**EPR and ENDOR.** Vanadyl–NC complexes were prepared by mixing together the desired quantity of NC in 0.03 M Pipes buffer at pH 5.8 with  $\text{VO}_2\text{SO}_4$  in a small quantity of  $\text{H}_2\text{O}$  or  $^2\text{H}_2\text{O}$ .  $\text{VO}^{2+}$  was added under a nitrogen atmosphere. For EPR and ENDOR studies, the final concentration of NC was 1 mM, while the metal ion concentration varied from 0 to 12 mM. All solutions were purged with nitrogen gas and stored frozen in EPR sample tubes to prevent oxidation.

EPR and ENDOR spectra were recorded with use of X-band Bruker ER200D or ESP 300E spectrometers with ENDOR accessories, as described (15–18). The ESP 300E spectrometer is equipped with a complete computer interface (ESP 3220 data system) for spectrometer control, data acquisition and processing, and communications. A cylindrical  $\text{TM}_{110}$  cavity with a 17-turn bronze wire helix mounted on the quartz dewar insert of the Oxford Instruments liquid helium cryostat (ESR910) was used for both EPR and ENDOR. A Wavetek signal generator (model 3000) was used to produce a frequency-modulated, amplitude-controlled radio frequency (rf), and an Electronic Navigation Industries rf power amplifier (model A500) was used in the final amplification stage. The sample temperature was controlled by an Oxford Instruments temperature controller (model ITC4). Typical experimental conditions for EPR measurements were as follows: sample temperature, 20 K; microwave frequency, 9.45 GHz; incident microwave power, 64  $\mu\text{W}$  (full power, 640 mW at 0 dB); modulation frequency, 12.5 kHz; modulation amplitude, 0.8 G; and for ENDOR measurements: microwave power, 6.4 mW; rf power, 50–70 W; rf modulation frequency, 12.5 kHz; and rf modulation depth,  $\leq 30$  kHz. The static laboratory magnetic field was not modulated for ENDOR.

## RESULTS

**Properties of NC.** For the characterization of metal-binding properties, we have employed the  $\text{VO}^{2+}$  ion as a paramagnetic substitute for  $\text{Ca}^{2+}$  in binding to the native protein. It

Table 1. Properties of bovine NC-A

Molecular weight	$14 \times 10^3$ (as a monomer)
Dissociation constant toward COM	$7.7 \times 10^{-7}$ M
Carbohydrate content	11.5 wt%
Phosphate content	11.7 mol/mol of protein

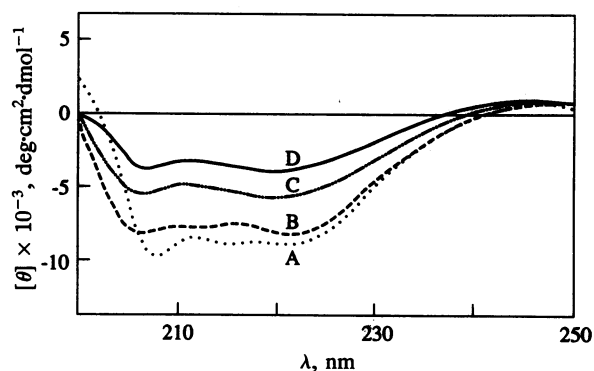


FIG. 1. CD spectra of metal-free NC-A and NC-A complexed to  $\text{VO}^{2+}$  and  $\text{Ca}^{2+}$  ions. The spectra are shown for the following samples: A, metal-free NC ( $\cdots$ ); B,  $[\text{VO}^{2+}]:[\text{NC}]$  molar ratio of 1:1 ( $---$ ); C,  $[\text{VO}^{2+}]:[\text{NC}]$  molar ratio of 4:1 ( $- \cdot - \cdot -$ ); and D,  $[\text{Ca}^{2+}]:[\text{NC}]$  molar ratio of 4:1 ( $---$ ).

was necessary, therefore, to determine whether substitution of  $\text{Ca}^{2+}$  by  $\text{VO}^{2+}$  in NC induces structural or conformational alterations different from those induced by  $\text{Ca}^{2+}$  binding. Fig. 1 illustrates the CD spectra of metal-free NC, normal  $\text{Ca}^{2+}$ -bound NC, and  $\text{VO}^{2+}$ -reconstituted NC at different molar ratios of  $\text{VO}^{2+}:\text{NC}$ . No further change was observed in the CD spectra at  $[\text{VO}^{2+}]:[\text{NC}]$  or  $[\text{Ca}^{2+}]:[\text{NC}]$  molar ratios greater than 4:1. If one assumes a value of the molar ellipticity  $[\Theta]$  of  $-33.6 \times 10^3 \text{ deg-cm}^2\text{-dmol}^{-1}$  at 220 nm for 100%  $\alpha$ -helical structure of the polypeptide backbone (19), then

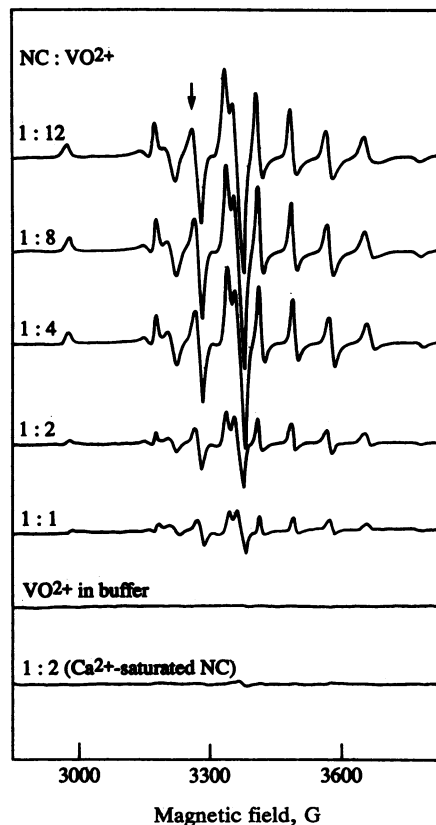


FIG. 2. First-derivative EPR spectra of  $\text{VO}^{2+}$ -NC complexes in frozen aqueous solution. The solutions were buffered to pH 5.8 with 0.03 M Pipes. The spectra were recorded under identical spectrometer settings with different  $\text{NC}:\text{VO}^{2+}$  molar ratios as indicated. The final NC concentration was 1 mM. Only a part of the EPR spectra is shown here. (The EPR features at the extreme left and right are from the  $-5/2$  and  $+3/2$  parallel components, respectively; see ref. 15.) The  $-3/2$  perpendicular EPR feature is indicated by an arrow.

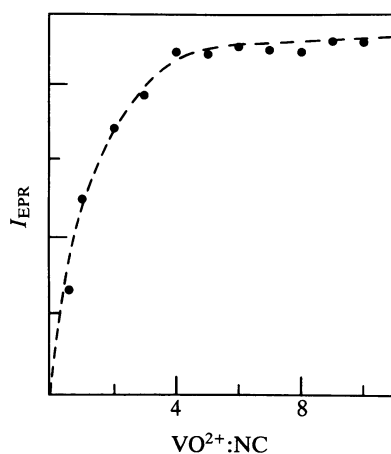


FIG. 3. EPR spectrometric titration of the  $\text{VO}^{2+}$  ion complexed to NC. The EPR signal intensities of the  $-3/2$  perpendicular line (see Fig. 2) of  $\text{VO}^{2+}$  are plotted as a function of  $\text{VO}^{2+}:\text{NC}$  ratio. Dashed lines are drawn through the experimentally measured points.

metal-free NC is composed of 30%  $\alpha$ -helical structure. Correspondingly, the helical content of NC saturated with  $\text{VO}^{2+}$  is about 16% and it is about 12% with  $\text{Ca}^{2+}$ . The small difference in CD of  $\text{VO}^{2+}$ -saturated NC and  $\text{Ca}^{2+}$ -saturated NC can be seen in spectra C and D, respectively, in Fig. 1. This difference is probably due to the presence of ligand-to-metal charge transfer transitions that are expected to occur for  $\text{VO}^{2+}$  as an open shell metal cation, particularly with oxygen-donor ligands (20), in contrast to the closed shell character of  $\text{Ca}^{2+}$ . This prevents further quantitative analysis of CD spectra. However, the change in CD for different molar ratios of  $\text{VO}^{2+}:\text{NC}$  was parallel to that for  $\text{Ca}^{2+}:\text{NC}$ . The similarity in spectra C and D indicates that a similar conformational change is induced in NC upon binding 4 equivalents of  $\text{VO}^{2+}$  as for  $\text{Ca}^{2+}$ . Evidence for competitive binding of  $\text{VO}^{2+}$  with  $\text{Ca}^{2+}$  is given below.

**EPR of  $\text{VO}^{2+}:\text{NC}$ : Stoichiometry of Vanadyl-NC Binding.** In the  $\text{V}^{4+}$  ion with a  $3d^1$  configuration, the unpaired electron is strongly coupled to the ( $I = 7/2$ )  $^{51}\text{V}$  nucleus. In frozen solution, the  $\text{VO}^{2+}$  ion is characterized by an axially symmetric  $g$  matrix and exhibits eight parallel and eight perpendicular absorption lines (21, 22). Fig. 2 illustrates the EPR spectra of  $\text{VO}^{2+}:\text{NC}$  complexes. Since at neutral pH free  $\text{VO}^{2+}$  forms an EPR-silent, polymeric  $\text{VO}(\text{OH})_2$  species (23), the peak-to-peak amplitude is proportional only to the amount of NC-bound  $\text{VO}^{2+}$ . An increase in signal amplitude was observed up to a  $\text{VO}^{2+}:\text{NC}$  molar ratio of 4:1. Moreover, when  $\text{VO}^{2+}$  was added to  $\text{Ca}^{2+}$ -saturated NC-A, as seen in the bottom-most trace of the complex with a  $\text{VO}^{2+}:\text{NC}$  ratio of 2:1, the trace was similar to that of  $\text{VO}^{2+}$  in buffer alone, indicating that  $\text{VO}^{2+}$  is bound only at the same sites as  $\text{Ca}^{2+}$ .

Fig. 3 illustrates a plot of the peak-to-peak amplitude of the  $-3/2$  perpendicular EPR feature as a function of the  $\text{VO}^{2+}:\text{NC}$  ratio. The  $-3/2$  perpendicular resonance feature was selected to monitor the stoichiometry of  $\text{VO}^{2+}$  binding since it has virtually no overlap with nearby parallel EPR transitions. Fig. 3 shows an increase in signal intensity up to a  $\text{VO}^{2+}:\text{NC}$  ratio of 4:1, after which the signal intensity remains constant, indicating that the stoichiometry of  $\text{VO}^{2+}$  binding to NC-A is 4:1. A similar conclusion concerning the stoichiometry of  $\text{Ca}^{2+}$  binding to NC was drawn on the basis of  $^{31}\text{P}$  NMR studies of  $\text{Ca}^{2+}:\text{NC}$  complexes and on the basis of equilibrium dialysis of the native NC with  $^{45}\text{Ca}$  (6).

**Coordination Environment of  $\text{VO}^{2+}$  Ion in NC.** To identify the origin of the ligands directly coordinated to the  $\text{VO}^{2+}$  when bound to NC, we have carried out both EPR and ENDOR studies. The principal hyperfine (hf) values  $A_{\parallel}$  and  $A_{\perp}$  for the vanadium nucleus and the values of  $g_{\parallel}$  and  $g_{\perp}$  reflect the environment of the metal ion in the vanadyl complexes (7). In Table 2 we compare EPR parameters of  $\text{VO}^{2+}:\text{NC}$  complexes to those of other  $\text{VO}^{2+}$  complexes containing oxygen, nitrogen, and sulfur ligands in the equatorial plane. Since  $g_{\parallel}$  depends primarily on the donor-ligand atoms in the equatorial plane (7), the values of  $g_{\parallel}$  are the most useful guide for comparing different environments. The results show that the EPR parameters of  $\text{VO}^{2+}:\text{NC}$  complexes are most similar to those of  $\text{VO}^{2+}$  complexes with oxygen-donor ligands in the equatorial plane.

Changes in EPR linewidths can also be analyzed to yield information about the symmetry and coordination environment of a  $\text{VO}^{2+}$  ion (22). For the solvated vanadyl ion, the EPR linewidth decreases upon introduction of perdeuterated solvents, showing an approximate 6 G decrease in the linewidth of the  $-3/2$  perpendicular resonance feature with four equatorially located, inner-sphere coordinated water molecules (15, 22). In Fig. 4, we illustrate the  $-3/2$  perpendicular EPR feature of  $\text{VO}^{2+}$  ion complexed to NC. In the natural-abundance solvent, the linewidth changed only from  $14.10 \pm 0.32$  G to  $14.30 \pm 0.30$  G when the  $\text{VO}^{2+}:\text{NC}$  molar ratio was changed from 1:1 to 4:1. In the perdeuterated solvent, the linewidth is found to be identical, as seen in the bottom-most spectrum and as listed in Table 2. These results suggest that in the  $\text{VO}^{2+}:\text{NC}$ -A complex no solvent molecule is directly coordinated to the  $\text{VO}^{2+}$  ion as an equatorial ligand. Definitive proof of the absence of inner-sphere coordinated solvent molecules relies on the ENDOR studies, which are discussed below.

ENDOR can detect superhyperfine couplings of nearby nuclei with a greater sensitivity than EPR. For a system of low  $g$  anisotropy, as in the case of the  $\text{VO}^{2+}$  ion,  $^1\text{H}$  ENDOR features appear symmetrically about the proton Larmor frequency. Moreover, the axial character of the vanadyl ion allows one to assign by ENDOR the spatial disposition of coordinating ligands as equatorial or axial (12, 15, 24).

Table 2. Comparison of EPR parameters of  $\text{VO}^{2+}$  complexes

Complex	$g_{\parallel}$	$g_{\perp}$	$A_{\parallel}^*$	$A_{\perp}^*$	$\Delta H_{pp}^{\dagger}$	Source or ref.
$[\text{VO}^{2+}:\text{NC}]$	1.940	1.989	535.4	193.5	14.30 (14.32)	This work
$[\text{VO}(\text{H}_2\text{O})_5]^{2+}$	1.933	1.978	547.4	211.9	12.30 (6.15)	22
$[\text{VO}(\text{acac})_2]$ in THF	1.945	1.981	506.7	183.3	—	21
$[\text{VO}(\text{TPP})]$ in THF	1.964	1.989	477.0	162.4	—	21
$[\text{VO}(\text{S}_2\text{O}_2)]^{\ddagger}$	1.969	1.979	443.5	184.6	—	7

acac, Acetylacetonate; THF, tetrahydrofuran; TPP, tetraphenylporphyrin.

\*hf values are given in units of MHz.

$^{\dagger}$ The EPR linewidths of the  $-3/2 \perp$  feature are given in units of gauss. Values in parentheses are for complexes in deuterated solvents. For NC, EPR linewidths are given for the complexes with a  $\text{VO}^{2+}:\text{NC}$  molar ratio of 4:1.

$^{\ddagger}$ Extracted from ref. 7 for  $\text{VO}^{2+}$  complexes with two oxygen-donor and two sulfur-donor ligands in the equatorial plane.

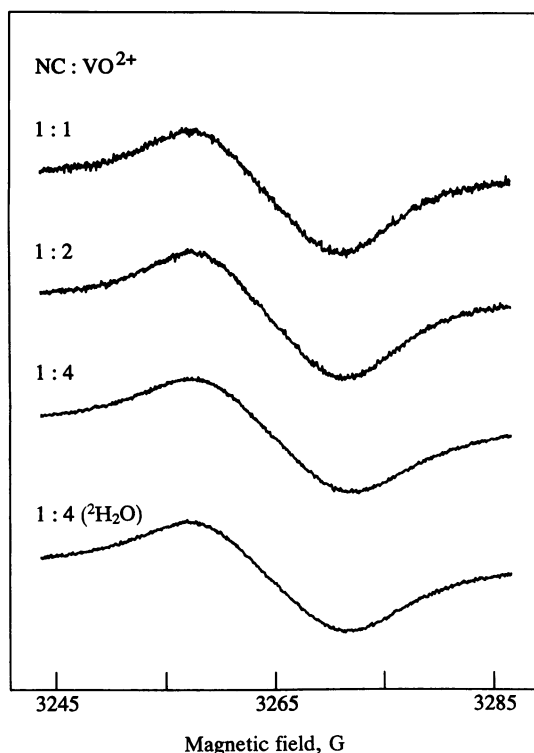


FIG. 4. Comparison of the linewidth of the  $-3/2$  perpendicular EPR feature for the  $\text{VO}^{2+}$  ion complexed to NC at different NC: $\text{VO}^{2+}$  ratios in frozen solutions of natural and perdeuterated water. The solutions were buffered to pH 5.8.

Fig. 5 compares the proton ENDOR spectra of  $\text{VO}^{2+}$  complexed to NC-A at different molar ratios in natural abundance and perdeuterated solvents and to that of the free, solvated  $\text{VO}^{2+}$  ion. For the free  $\text{VO}^{2+}$  ion, the proton ENDOR features from the coordinated water molecules are indicated in the uppermost spectrum for both the axial and the equatorial positions. These assignments are based on our previous ENDOR studies of the solvation structure of  $\text{VO}^{2+}$  (15). In the ENDOR spectra of the  $\text{VO}^{2+}$ -NC complexes, no proton resonance feature was observed that corresponded to either axially or equatorially bound water in the inner coordination sphere. Moreover, identical results are observed for different metal:protein ratios, indicating that there is no inner-sphere coordinated water in all four metal-binding sites. However, in  $\text{VO}^{2+}$ -NC complexes, other ENDOR features are observed, as seen in spectra B1 and B2 in Fig. 5. Since all of these ENDOR features were also observed for  $\text{VO}^{2+}$ -NC complexes in perdeuterated solvent, as seen in spectrum B3, these features must come from nonexchangeable protons of protein residues. Although spectrum B3 shows a diminution of the ENDOR feature in the matrix region centered at the proton Larmor frequency, this difference is due to distant, weakly coupled exchangeable protons from solvents in the outer coordination sphere or from protons further removed from the  $\text{VO}^{2+}$  ion (15).

## DISCUSSION

The  $\text{Ca}^{2+}$ -binding proteins that have been characterized by high-resolution x-ray crystal structure analysis fall into two general categories (25). One group includes many extracellular enzymes and proteins that have enhanced thermal stability or resistance to proteolytic degradation as a result of binding  $\text{Ca}^{2+}$  (26, 27). The other group is made up of a family of intracellular proteins that reversibly bind  $\text{Ca}^{2+}$ . The second group is distinguished from the first in that its members

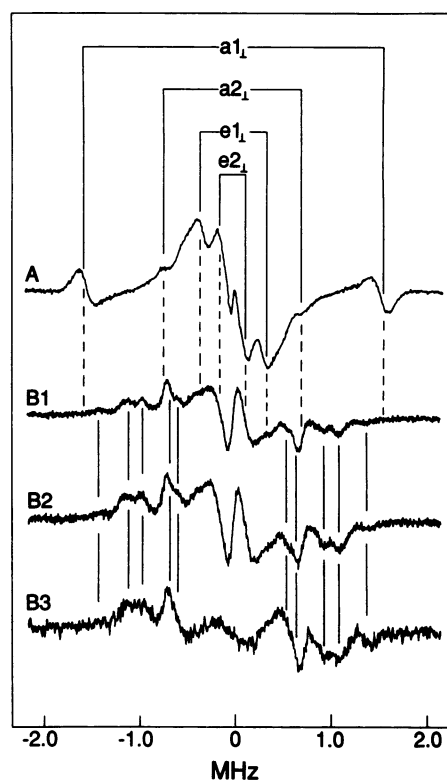


FIG. 5. Proton ENDOR spectra of the  $\text{VO}^{2+}$  complexes in frozen aqueous solution. The spectra are shown for the following samples in top-to-bottom order: A,  $\text{VO}(\text{H}_2\text{O})_5^{2+}$  complex,  $\text{VO}^{2+}$  in  $\text{H}_2\text{O}/\text{C}_2\text{H}_5\text{OH}$  cosolvent mixture; B1,  $\text{VO}^{2+}$ -NC complex (1:1 molar ratio of  $\text{VO}^{2+}$ :NC) in aqueous buffer; B2,  $\text{VO}^{2+}$ -NC complex (4:1 molar ratio of  $\text{VO}^{2+}$ :NC) in aqueous buffer; and B3,  $\text{VO}^{2+}$ -NC complex (4:1 molar ratio of  $\text{VO}^{2+}$ :NC) in perdeuterated aqueous buffer. The magnetic field was set to  $-3/2$  perpendicular EPR line at about 3265 G (see Figs. 2 and 4). The ENDOR line pairs were equally spaced about the free proton frequency of 13.86 MHz. The abscissa indicates the ENDOR shift (measured ENDOR frequency minus free proton Larmor frequency). In the top spectrum, proton ENDOR features from inner coordinated water molecules in the axial and equatorial positions, labeled as  $a_1$ ,  $a_2$  and  $e_1$ ,  $e_2$ , respectively, are identified in the stick diagram. The ENDOR features that are seen in the uppermost spectrum do not appear in the spectra of B1-B3 for the  $\text{VO}^{2+}$  ion complexed to NC, indicated by dashed lines. The new resonance features appearing in spectra B1-B3 of  $\text{VO}^{2+}$ -NC complexes are indicated by solid lines.

have a common  $\text{Ca}^{2+}$ -binding helix-loop-helix motif, termed an "EF-hand" that has been widely applied to describe  $\text{Ca}^{2+}$ -binding sites (28, 29). NC is similar to the proteins of the second group because it reversibly binds  $\text{Ca}^{2+}$ .

Although the primary sequence of NC has not yet been determined, amino acid analysis shows the presence of a high content of Asp and Glu (4). These residues may provide an ideal electrostatic environment for  $\text{Ca}^{2+}$  binding, as observed in other  $\text{Ca}^{2+}$ -binding proteins (30). Although, NC contains two His residues (4), no  $^{14}\text{N}$  ENDOR feature is detected even at 4 K attributable to a vanadyl-coordinated imidazole ring. Therefore, on the basis of our ENDOR results and the EPR results shown in Table 2, it is very unlikely that histidine is involved in metal binding. Also, only two Cys residues are found in NC and they are cross-linked by a disulfide bond.‡

‡Cysteine residues were determined either by carboxymethylation of SH- groups using iodoacetamide after mercaptoethanol reduction and quantitated as *S*-carboxymethyl cysteine or by oxidation of cysteine in performic acid and measured as cysteic acid after hydrolysis in 6 M HCl for 24 hr, with a Beckman model 119C amino acid analyzer (Y.N., unpublished results).

Moreover, the EPR parameters in Table 2 are not compatible with a sulfur-donor environment. Since the electrostatic energy term ( $Z/r$ ) is similar for  $\text{Ca}^{2+}$  and  $\text{V}^{4+}$  (31) and both  $\text{Ca}^{2+}$  and  $\text{VO}^{2+}$  ions exhibit high affinity for binding to oxygen-donor ligands (7), it is likely that  $\text{VO}^{2+}$  binds tightly to  $\text{Ca}^{2+}$  sites in proteins. Competitive binding of  $\text{VO}^{2+}$  and  $\text{Ca}^{2+}$  to NC demonstrated by EPR indicates that  $\text{VO}^{2+}$  specifically binds to the same sites as does  $\text{Ca}^{2+}$ . Although in  $\text{VO}^{2+}$ , one coordination position is occupied by the vanadyl oxygen, the vanadium atom can accommodate up to six ligands beyond the oxo ( $\text{O}^{2-}$ ) group (32). As observed in CD spectra in Fig. 1, both  $\text{Ca}^{2+}$  and  $\text{VO}^{2+}$  binding induced similar conformational changes in NC. In the absence of metal ions, the electrostatic repulsion between the coordinating oxygen ligands may cause significant structural perturbation.

NC, as described in this report, differs from other known  $\text{Ca}^{2+}$ -binding proteins: (i) Water does not appear to be accommodated into the inner-coordination sphere in its metal-binding sites, as is commonly observed for other  $\text{Ca}^{2+}$ -binding proteins (30); and (ii) NC exhibits tighter  $\text{Ca}^{2+}$ -binding affinity compared to other  $\text{Ca}^{2+}$ -binding proteins. The tighter binding of  $\text{Ca}^{2+}$  ions in NC ( $K_d < 10^{-7}$  M) may be responsible for the exclusion of inner-sphere water. In this respect, NC can be compared with the carp muscle  $\text{Ca}^{2+}$ -binding protein parvalbumin (33, 34). Parvalbumin contains two  $\text{Ca}^{2+}$ -binding sites, one of which is a high-affinity site with a dissociation constant of  $<10^{-7}$  M, similar to that of NC. In this  $\text{Ca}^{2+}$ -binding site there are six oxygen-donor ligands from protein residues, and there is complete exclusion of inner-sphere water (34). The tighter binding site in parvalbumin, with its highly charged residues located within a hydrophobic environment, favors metal binding (35). The strong binding of  $\text{Ca}^{2+}$  ions with oxygen-donor ligands in NC, as in parvalbumin, may provide a similar electrostatic environment for metal binding. The highly charged oxygen-donor ligands may be responsible for the complete exclusion of water from the inner-coordination sphere.

On the basis of EPR and ENDOR studies of  $\text{VO}^{2+}$ -NC complexes, we have also shown that all four metal-binding sites in NC-A are similar to each other. Preliminary EPR studies of NC-C purified from bovine kidney tissue show two classes of nonequivalent  $\text{Ca}^{2+}$ -binding sites. This fraction of NC serves as a model for the human protein from patients with stone-forming tendencies (3-5). Differences in the affinity of  $\text{Ca}^{2+}$  binding corresponding to fractions characterized as strong and weak inhibitors and differences in its coordination structures may reflect functional properties. Further investigations to clarify these relationships are needed.

We thank Professors M. W. Makinen and F. L. Coe for helpful discussions and support. This work was supported by grants from the National Institutes of Health (GM 21900 and AM 33949).

- Nakagawa, Y., Abram, V., Kezdy, F. J., Kaiser, E. T. & Coe, F. L. (1983) *J. Biol. Chem.* **256**, 3936-3944.
- Nakagawa, Y., Abram, V., Parks, J. H., Lau, H. S.-H., Kawooya, J. K. & Coe, F. L. (1985) *J. Clin. Invest.* **76**, 1455-1462.
- Nakagawa, Y., Ahmed, M., Hall, S. L., Deganello, S. & Coe, F. L. (1987) *J. Clin. Invest.* **79**, 1782-1787.
- Nakagawa, Y., Renz, C. L., Ahmed, M. & Coe, F. L. (1991) *Am. J. Physiol.* **260**, F243-F248.
- Nakagawa, Y., Abram, V. & Coe, F. L. (1984) *Am. J. Physiol.* **247**, F765-F772.
- Nakagawa, Y., Otsuki, T. & Coe, F. L. (1985) *FEBS Lett.* **250**, 187-190.
- Chasteen, N. D. (1981) in *Biological Magnetic Resonance*, eds. Berliner, L. J. & Reuben, J. (Plenum, New York), Vol. 3, pp. 53-119.
- Chasteen, N. D., DeKoch, R. J., Roggers, B. L. & Hanna, M. W. (1973) *J. Am. Chem. Soc.* **95**, 1301-1309.
- DeKoch, R. J., West, D. J., Cannon, J. C. & Chasteen, N. D. (1974) *Biochemistry* **13**, 4347-4354.
- Chasteen, N. D. (1983) *Struct. Bonding (Berlin)* **53**, 105-138.
- Ahmed, R. H., Nieves, J., Kim, L., Echegoyen, L. & Puett, D. (1987) *J. Protein Chem.* **6**, 431-439.
- Mustafi, D., Telsler, J. & Makinen, M. W. (1992) *J. Am. Chem. Soc.* **114**, 6219-6226.
- Ames, B. N. (1966) *Methods Enzymol.* **8**, 115-118.
- Clamp, J. R., Bhatti, T. & Chamber, R. E. (1971) *Methods Biochem. Anal.* **19**, 229-344.
- Mustafi, D. & Makinen, M. W. (1988) *Inorg. Chem.* **27**, 3360-3368.
- Yim, M. B. & Makinen, M. W. (1986) *J. Magn. Reson.* **70**, 89-105.
- Mustafi, D., Sachleben, J. R., Wells, G. B. & Makinen, M. W. (1990) *J. Am. Chem. Soc.* **112**, 2558-2566.
- Mustafi, D., Boisvert, W. E. & Makinen, M. W. (1993) *J. Am. Chem. Soc.* **115**, 3674-3682.
- Woody, R. W. (1968) *J. Chem. Phys.* **49**, 4797-4806.
- Ballhausen, C. J. & Gray, H. B. (1961) *Inorg. Chem.* **1**, 111-122.
- Kivelson, D. & Lee, S.-K. (1964) *J. Chem. Phys.* **41**, 1896-1903.
- Albanese, N. F. & Chasteen, N. D. (1978) *J. Phys. Chem.* **82**, 910-914.
- Francavilla, J. & Chasteen, N. D. (1975) *Inorg. Chem.* **14**, 2860-2862.
- Makinen, M. W. & Mustafi, D. (1994) in *Metal Ions in Biological Systems*, ed. Sigel, H. (Dekker, New York), Vol. 31, pp. 89-127.
- Strynadka, N. C. J. & James, M. N. G. (1989) *Annu. Rev. Biochem.* **58**, 951-998.
- Dijkstra, B. W., Kalk, K. H., Hol, W. G. J. & Drenth, J. (1981) *J. Mol. Biol.* **147**, 97-123.
- McPhalen, C. A., Svendsen, I., Jonassen, I. & James, M. N. G. (1985) *Proc. Natl. Acad. Sci. USA* **82**, 7242-7246.
- Babu, Y. S., Bugg, C. E. & Cook, W. J. (1985) *J. Mol. Biol.* **204**, 191-204.
- Herzberg, O. & James, M. N. G. (1985) *Nature (London)* **313**, 653-659.
- Glusker, J. (1991) *Adv. Protein Chem.* **42**, 1-76.
- Williams, R. J. P. (1985) *Eur. J. Biochem.* **150**, 231-248.
- Posner, B. I., Faure, R., Burgess, J. W., Bevan, A. P., Lachance, D., Zhang-Sun, G., Fantus, I. G., Ng, J. B., Hall, D. A., Lum, B. S. & Shaver, A. (1994) *J. Biol. Chem.* **269**, 4596-4604.
- Coffee, C. J. & Bradshaw, R. A. (1973) *J. Biol. Chem.* **248**, 3305-3312.
- Kretsinger, R. H. & Nockolds, C. E. (1973) *J. Biol. Chem.* **248**, 3313-3326.
- Yamashita, M. M., Wesson, L., Eisenman, G. & Eisenberg, D. (1990) *Proc. Natl. Acad. Sci. USA* **87**, 5648-5652.